

# A Conceptual Model for the Treatment of Ammonia Vapors in a Biotrickling Filter

Paper #690

Sakuma T,<sup>1,2</sup> Aoki M,<sup>2</sup> Hattori T,<sup>2</sup> Gabriel D,<sup>3</sup> Deshusses M.A.<sup>1</sup>

<sup>1</sup>Department of Chemical and Environmental Engineering, University of California Riverside, CA 92521

<sup>2</sup>Aisin Takaoka Co., Ltd, Toyota City, Japan

<sup>3</sup>Department of Chemical Engineering, ETSE, Universitat Autònoma de Barcelona, Spain

## ABSTRACT

A dynamic model for describing the behavior of a biotrickling filters for the treatment of the ammonia odor was developed. At this time, the model was not validated, but independent experiments will later serve to calibrate the model, so that it can be further validated with dynamic and steady-state data from a pilot-scale biotrickling filter. The field biotrickling filter was able to treat up to 3.45 g of ammonia  $\text{m}^{-3} \text{h}^{-1}$  with essentially 98% removal, but unstable operation and accumulation of nitrite stimulated the modeling effort. In the future, model simulations will allow to determine the influence of selected parameters on the removal efficiency of ammonia. Of particular importance, was to include in the model the inhibitory effect of free ammonia and free nitric acid on nitrification, i.e., the conversion of ammonia to nitrite and on the nitrification, i.e., the conversion of nitrite to nitrate. The model also includes gas-liquid mass transfer of ammonia, and detailed biokinetic relationships to account for all biological inhibitions encountered during nitrification. When fully developed, the model is expected to be a significant support for the design and operation of biotrickling filter for ammonia control.

## INTRODUCTION

Ammonia emissions are very common in operations such as composting, and intensive pig or cow farming. Ammonia has a moderate odor threshold and emissions are regulated both because of odor and air pollution concerns. Ammonia can be easily scrubbed chemically, though the costs of chemical scrubbing can be significant as ammonia emissions are usually associated with very large air flows. Another disadvantage of chemical scrubbing is that it results in large amounts of an acidic ammonium solution that needs to be disposed of.

Biotreatment is an interesting alternative, as the complexity of the nitrogen cycle offers several possibilities as far as the ultimate fate of the nitrogen is concerned (nitrification to nitrite or nitrate, followed by denitrification to nitrogen gas). However, many reports on ammonia biotreatment in biofilters or biotrickling filters have identified bacteria inhibition as one of the factors limiting the long-term performance and reliability of ammonia biotreatment. This is because ammonia treatment involves various microorganisms thriving under specific conditions.

Achieving successful nitrification and denitrification requires a careful balance of the conditions such as pH, pollutant-substrate concentrations, dissolved oxygen, etc. Of particular importance, is the inhibitory effect of free ammonia (FA) and free nitric acid (FNA) on nitrification, i.e., the conversion of ammonia to nitrite and on the nitrification, i.e., the conversion of nitrite to nitrate. Since biofilters and biotrickling filters are often operated with a minimum of free water and/or of feed of fresh recycle liquid, the concentrations of FA, FNA can quickly reach inhibitory levels while pH swings can affect the microflora.

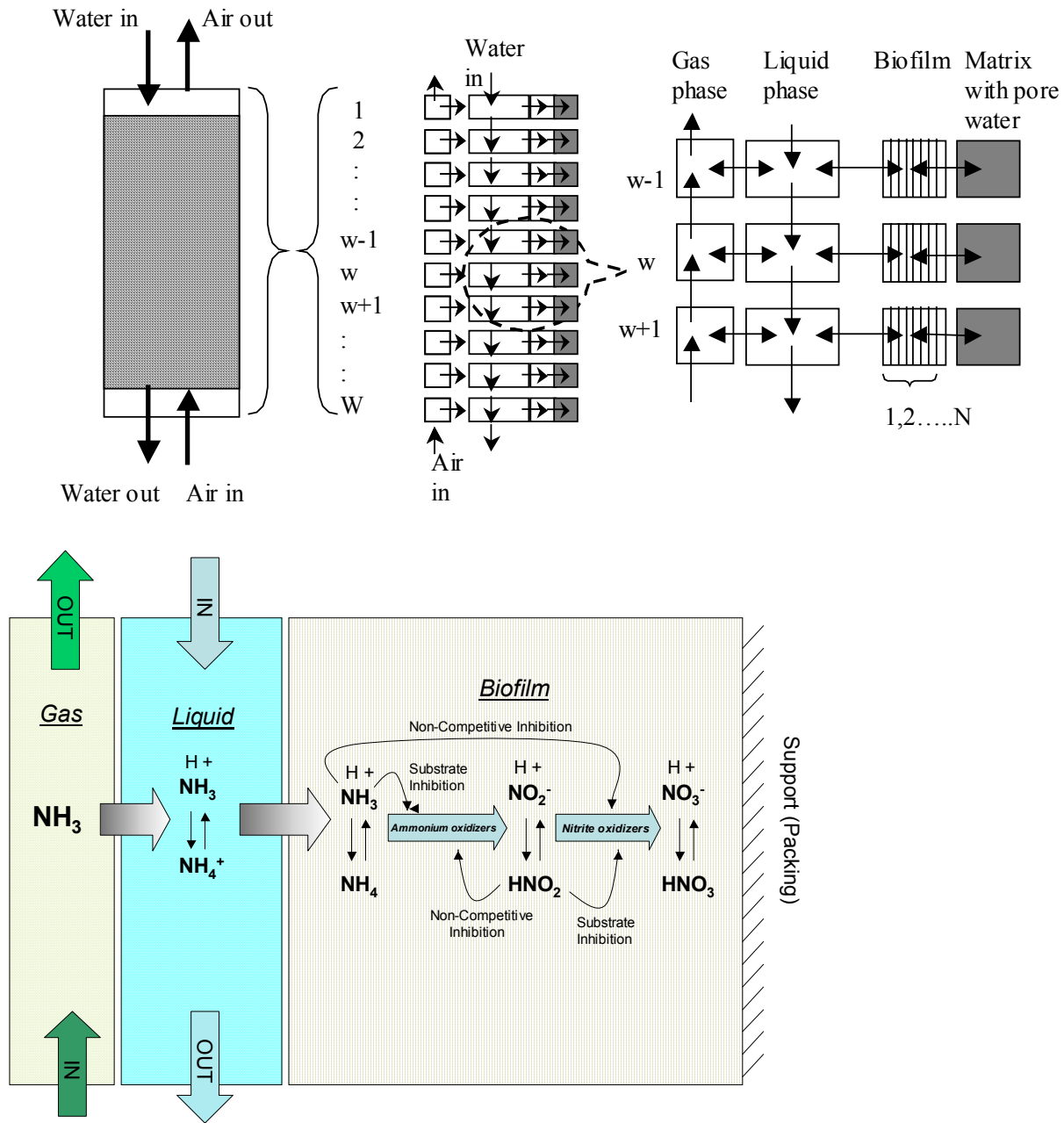
In the present paper, a conceptual model of a biotrickling filter was developed. The model includes gas-liquid mass transfer of ammonia, and detailed biokinetic relationships to account for all biological inhibitions encountered during nitrification. The model also includes a denitrification step conducted in a separate vessel, as the ultimate objective is to absorb and nitrify ammonia in the biotrickling filter, and denitrify the produced nitrate and nitrite in the biotrickling filter sump or in an ancillary vessel. Ultimately, it is expected that the model will help size biotrickling filter and denitrification reactors, as well as optimize conditions such as trickling rate, and feeding of carbon source for denitrification. One can also speculate that the model could be used for process control, in an expert system, as is being done in wastewater treatment plants.

At this stage, the work is ongoing and only partial results are available. Model parameters were for most taken from previous studies related to wastewater treatment. This will be refined later. Still, the model is presently being evaluated for several different purposes which are briefly reviewed and discussed. One is the optimization an existing pilot biotrickling filter treating ammonia at a pig farm in Japan. The pilot biotrickling filter has been operated for several months, with slowly decreasing performance, accumulation of nitrite, and unsatisfactory denitrifying activity. Remedial actions were proposed based on early model simulations. The model can also be used to evaluate alternative designs of biotrickling filters for ammonia removal, and to optimize operation of the biotrickling filters, in particular the frequency of intermittent trickling, and the supply of fresh liquid. It is also expected that when fully functional, the model could also be used to support the design of new packings for biotrickling filters specific for ammonia control. Detailed results will be presented and discussed in follow up publications.

## **MODEL DEVELOPMENT**

The biotrickling filter model is based on dynamic mass balances and the simulation techniques described by Dunn et al. (4) and Ingham et al. (5) combined with the detailed modeling of the nitrification process described by Carrera *et al.* (3). A schematic of the model concept is shown in Figure 1. For mass balance purposes, the biotrickling filter is divided into layers in the axial direction. Within each layer, four phases are considered for mass balances: the gas phase, the liquid phase, the biofilm and pore water. The biofilm thickness is further divided into N layers perpendicular to the flux of pollutant.

**Figure 1.** Schematic of model concept. Top: reactor discretization (sump with denitrification tank not shown), bottom, details of ammonia fate.



To describe the phenomena that occur in the biotrickling filter, the following assumptions are made:

1. Each subdivision shown in Figure 1 is ideally mixed. This is a reasonable assumption if the number of elements is large.
2. The biofilm is treated as a planar surface and the biomass is homogeneously distributed in the biofilm, and throughout the bioreactor. These assumptions are commonly made when modeling biofilm reactors because of the lack of information on the biofilm architecture and on the spatial distribution of pollutant-degrading organisms.
3. Water in the bioreactor is divided between free trickling water which volume is equal to the dynamic holdup, and pore water which volume equals the static holdup.
4. Adsorption of the treated compound to the matrix can be neglected. This has been verified experimentally.
5. Transfer between the gas and liquid phase is described by an overall mass transfer coefficient  $K_{ol}$ .
6. The kinetics for ammonia, nitrite and nitrate conversion in the biofilm are described by modified Michaelis-Menten equations with substrate inhibitions, as described by Carrera et al. (3). The no-growth assumption is reasonable since the growth rate of ammonia degraders is usually very slow, so the biomass content can be assumed to be essentially constant.
7. Biodegradation occurs in the biofilm only. This is reasonable as the density of organisms in the trickling liquid is very low, and pores in the porous packing are too small to allow for significant biomass colonization.
8. The biofilm is assumed to have the same physicochemical properties (Henry coefficient, diffusion coefficient, acid-base equilibrium) as water.
9. Denitrification occurs in a separate tank, where the trickling liquid is collected. The denitrification tank is assumed to be ideally mixed.

## Mass Balances

### Gas phase

$$V_{gw} \frac{dC_{NH_3} g[w]}{dt} = G(C_{NH_3} g[w+1] - C_{NH_3} g[w]) - J_{g_{NH_3}}[w] \quad (1)$$

where  $V_{gw}$  is the volume available for air flow in one layer,  $G$  is the total gas flow ( $m^3 h^{-1}$ ), and  $J_{g_{NH_3}}$  is that gas liquid mass transfer rate of ammonia (see Equation 11).

### Liquid phase

The dynamic mass balance for  $\text{NH}_3$  over a liquid segment in layer  $w$  is (note that reactions and reactions rates  $K_i$  are defined further):

$$Vlw \frac{dC_{\text{NH}_3}l[w]}{dt} = L(C_{\text{NH}_3}l[w-1] - C_{\text{NH}_3}l[w]) + Jg_{\text{NH}_3}[w] - A \times \frac{V}{W} \times Jb_{\text{NH}_3}[w] - K_{-1}(C_{\text{NH}_3}l[w] \times HH[w]) \times Vlw + K_1(C_{\text{NH}_4}l[w]) \times Vlw \quad (2)$$

where the array index  $w$  refers to the layer considered,  $C_{i,l}$  is the concentration of the species considered in the liquid,  $Vlw$  is the volume of free liquid in each horizontal subdivision,  $L$  is the total liquid flow rate ( $\text{m}^3 \text{h}^{-1}$ ),  $A$  is the specific interfacial area between gas and liquid phases or this between liquid and biofilm phases ( $\text{m}^2 \text{m}^{-3}$ ),  $V$  is the total volume of the bed ( $\text{m}^3$ ),  $W$  is the total number of layers, and  $K_j$  the reaction rate defined further.  $Jb_i$  is the flux of the substance  $i$  into the biofilm as described below by a finite difference expression of Fick's law applied to the liquid-biofilm interface (see Equation 10) and  $Jg_i$  is the flux of the substance  $i$  from the gas phase into the trickling liquid (Equation 11).

The dynamic mass balance for  $\text{NH}_4^+$  over a liquid segment in layer  $w$  is:

$$Vlw \frac{dC_{\text{NH}_4}l[w]}{dt} = L(C_{\text{NH}_4}l[w-1] - C_{\text{NH}_4}l[w]) - A \times \frac{V}{W} \times Jb_{\text{NH}_4}[w] + K_{-1}(C_{\text{NH}_3}l[w] \times HH[w]) \times Vlw - K_1(C_{\text{NH}_4}l[w]) \times Vlw \quad (3)$$

The dynamic mass balance for  $\text{NO}_2^-$  over a liquid segment in layer  $w$  is:

$$Vlw \frac{dC_{\text{NO}_2}l[w]}{dt} = L(C_{\text{NO}_2}l[w-1] - C_{\text{NO}_2}l[w]) - A \times \frac{V}{W} \times Jb_{\text{NO}_2}[w] + K_2(C_{\text{HNO}_2}l[w]) \times Vlw - K_{-2}(C_{\text{NO}_2}l[w] \times HH[w]) \times Vlw \quad (4)$$

The dynamic mass balance for  $\text{HNO}_2$  over a liquid segment in layer  $w$  is:

$$Vlw \frac{dC_{\text{HNO}_2}l[w]}{dt} = L(C_{\text{HNO}_2}l[w-1] - C_{\text{HNO}_2}l[w]) - A \times \frac{V}{W} \times Jb_{\text{HNO}_2}[w] - K_2(C_{\text{HNO}_2}l[w]) \times Vlw + K_{-2}(C_{\text{NO}_2}l[w] \times HH[w]) \times Vlw \quad (5)$$

The dynamic mass balance for  $\text{NO}_3^-$  over a liquid segment in layer  $w$  is:

$$Vlw \frac{dC_{\text{NO}_3}l[w]}{dt} = L(C_{\text{NO}_3}l[w-1] - C_{\text{NO}_3}l[w]) - A \times \frac{V}{W} \times Jb_{\text{NO}_3}[w] + K_3(C_{\text{HNO}_3}l[w]) \times Vlw - K_{-3}(C_{\text{NO}_3}l[w] \times HH[w]) \times Vlw \quad (6)$$

The dynamic mass balance for  $\text{HNO}_3$  over a liquid segment in layer  $w$  is:

$$Vlw \frac{dC_{HNO_3}l[w]}{dt} = L(C_{HNO_3}l[w-1] - C_{HNO_3}l[w]) - A \times \frac{V}{W} \times Jb_{HNO_3}[w] - K_3(C_{HNO_3}l[w]) \times Vlw + K_{-3}(C_{NO_3}l[w] \times HH[w]) \times Vlw \quad (7)$$

Mass balances are also written for  $[H^+]$  and dissolved oxygen, so that the effect of pH and oxygen limitations can be included.

The dynamic mass balance for  $H^+$  over a liquid segment in layer w is:

$$Vlw \frac{dC_{HH}l[w]}{dt} = L(C_{HH}l[w-1] - C_{HH}l[w]) - A \times \frac{V}{W} \times Jb_{HH}[w] + Vlw(K_1(C_{NH_4}l[w]) - K_{-1}(C_{NH_3}l[w] \times HH[w])) + Vlw(K_2(C_{HNO_2}l[w]) - K_{-2}(C_{NO_2}l[w] \times HH[w])) + Vlw(K_3(C_{HO_3}l[w]) - K_{-3}(C_{NO_3}l[w] \times HH[w])) \quad (8)$$

The dynamic mass balance for the dissolved oxygen DO over a liquid segment in layer w is:

$$Vlw \frac{dC_{DO}l[w]}{dt} = L(C_{DO}l[w-1] - C_{DO}l[w]) - A \times \frac{V}{W} \times Jb_{DO}[w] + Vlw \times Kga \times (CgO - C_{DO}l[w] \times mo) \times Vlw \quad (9)$$

As mentioned the interfacial fluxes of ammonia or oxygen are calculated using Fick's law on the liquid side of the interface:

$$Jb_i[w] = Di \times \left( \frac{dC_i}{dx} \right)_{x=0} = Di \times \frac{C_i l[w] - C_i b[w,1]}{\delta} \quad (10)$$

where  $Di$  is the effective diffusivity of the substance  $i$  in the biofilm,  $\delta$  is the thickness of one individual biofilm subdivision and is equal to the biofilm thickness divided by total number of biofilm segments  $N$ .  $C_i b[w,1]$  refers to the substance  $i$  in the first biofilm segment near the liquid interface, in layer  $w$  and  $C_i l$  is the concentration in the free liquid..

The transfer between the gas and the trickling liquid is described by mass transfer coefficient as in Equation 11. The transfer of substance  $i$  from the gas to the liquid is expressed as follow:

$$Jg_i[w] = Kga \times (C_i g[w] - C_i l[w] \times Hi) \times \frac{V}{W} \quad (11)$$

where  $Kga$  is the gas-liquid mass transfer coefficient multiplied by the specific interfacial area,  $C_i g$  and  $C_i l$  are the concentration of substance  $i$  in the gas and free liquid, respectively.  $Hi$  is the Henry constant of substance  $i$ .

### ***Biofilm phase.***

The concentrations of the various compounds in the biofilm are governed by diffusion and reaction equations. The mass balances for compound *i* in the first segment adjacent to the gas-liquid interface are described as follows:

$$A\delta \frac{V}{W} \frac{dC_i b[w,1]}{dt} = \frac{A}{\delta} \frac{V}{W} Di(C_i l[w] - 2C_i b[w,1] + C_i b[w,2]) + Reaction_i[w,1] A\delta \frac{V}{W} \quad (12)$$

where  $(A\delta V/W)$  is the volume of one biofilm subdivision,  $(AV/W)$  is its area normal to the diffusion flux, and  $\delta$  is its thickness.  $R_i$  is the biodegradation rate of ammonia or nitrite in each given  $[w, n]$  subdivision as described in Equations 16 and 17, respectively.

For the last segment next to the support material, the mass balances are

$$A\delta \frac{V}{W} \frac{dC_i b[w,N]}{dt} = \frac{A}{\delta} \frac{V}{W} Di(C_i b[w, N-1] - 2C_i b[w, N] + C_i p[w]) + Reaction_i[w, N] A\delta \frac{V}{W} \quad (13)$$

where  $C_{ip}$  is the concentration of substance *i* in the pore.

For all other segments, the mass balances are

$$A\delta \frac{V}{W} \frac{dC_i b[w,n]}{dt} = \frac{A}{\delta} \frac{V}{W} Di(C_i b[w, n-1] - 2C_i b[w, n] + C_i b[w, n+1]) + Reaction_i[w, n] A\delta \frac{V}{W} \quad (14)$$

### ***Pore water phase***

In a similar manner to the biofilm phase, mass balances are written for the substance *i* in the pore water. Consistent with Assumption 7, no biodegradation occurs in those segments. The pore water phase is essentially a dead volume, which is affecting the dynamic behavior of the model, but not its steady-state.

$$V_p W \frac{dC_i p[w]}{dt} = A \frac{V}{W} \frac{Di}{\delta} (C_i b[w, n] - C_i p[w]) + \text{Chemical Reactions} \quad (15)$$

where  $V_{pw}$  is the volume of the pore subdivision, and  $C_{ip}$  is the concentration of substance *i* in the pore.

### ***Biodegradation kinetics and oxygen uptake in the biofilm***

A modified Michaelis-Menten kinetic is used to describe the biodegradation of the contaminant, as the kinetics are expected to be affected by substrate and oxygen concentrations. Further, as described by Carrera et al (3), inhibitions are considered in the nitrification, i.e., the conversion of ammonia to nitrite ( $R_1$ ) and on the nitratation, i.e., the conversion of nitrite to nitrate ( $R_2$ )

$$R_1[w, n] = \frac{V_1 m \times C_{DO} b[w, n]}{K_{S1O2} + C_{DO} b[w, n]} \times \frac{C_{NH4} b[w, n]}{K_{SNH4} + C_{NH4} b[w, n] + \frac{C_{NH4} b[w, n]^2}{K_{I1NH4}}} \times \frac{K_{I1NO2}}{K_{I1NO2} + C_{NO2} b[w, n]} \quad (16)$$

$$R_2[w, n] = \frac{V_2 m \times C_{DO} b[w, n]}{K_{S2O2} + C_{DO} b[w, n]} \times \frac{C_{NO2} b[w, n]}{K_{SNO2} + C_{NO2} b[w, n] + \frac{C_{NO2} b[w, n]^2}{K_{I2NO2}}} \times \frac{K_{I2NH4}}{K_{I2NH4} + C_{NH4} b[w, n]} \quad (17)$$

in which  $V_m$  is the maximum degradation rate expressed per unit of biofilm volume ( $\text{g}_{\text{contaminants}} \text{m}^{-3} \text{biofilm} \text{h}^{-1}$ ). The different  $K_S$  values are the saturation constants and  $K_I$  values are the inhibition constants ( $\text{mol contaminant m}^{-3}$ ). The reaction for DO in biofilm segment  $[w, n]$  is given by:

$$\text{Reaction}_{DO} = -3 \times R_1 - R_2 \quad (18)$$

### ***Acid-base equilibrium reaction in the biofilm***

The reaction for  $\text{NH}_4^+$  in biofilm segment  $[w, n]$  is:

$$\text{Reaction}_{\text{NH}_4^+} = +K_{-1} \times C_{\text{NH}_3} b[w, n] \times C_{\text{HH}} b[w, n] - K_1 \times C_{\text{NH}_4} b[w, n] - R_1 \quad (19)$$

The reaction for  $\text{NH}_3$  in biofilm segment  $[w, n]$  is:

$$\text{Reaction}_{\text{NH}_3} = -K_{-1} \times C_{\text{NH}_3} b[w, n] \times C_{\text{HH}} b[w, n] + K_1 \times C_{\text{NH}_4} b[w, n] \quad (20)$$

The reaction for  $\text{NO}_2^-$  in biofilm segment  $[w, n]$  is:

$$\text{Reaction}_{\text{NO}_2^-} = +K_2 \times C_{\text{HNO}_2} b[w, n] - K_{-2} \times C_{\text{NO}_2} b[w, n] \times C_{\text{HH}} b[w, n] + R_1 - R_2 \quad (21)$$

The reaction for  $\text{HNO}_2$  in biofilm segment  $[w, n]$  is:

$$\text{Reaction}_{\text{HNO}_2} = -K_2 \times C_{\text{HNO}_2} b[w, n] + K_{-2} \times C_{\text{NO}_2} b[w, n] \times C_{\text{HH}} b[w, n] \quad (22)$$

The reaction for  $\text{NO}_3^-$  in biofilm segment  $[w, n]$  is:

$$\text{Reaction}_{\text{NO}_3^-} = +K_3 \times C_{\text{HNO}_3} b[w, n] - K_{-3} \times C_{\text{NO}_3} b[w, n] \times C_{\text{HH}} b[w, n] + R_2 \quad (23)$$

The reaction for  $\text{HNO}_3$  in biofilm segment  $[w, n]$  is:

$$\text{Reaction}_{\text{HNO}_3} = -K_3 \times C_{\text{HNO}_3} b[w, n] + K_{-3} \times C_{\text{NO}_3} b[w, n] \times C_{\text{HH}} b[w, n] \quad (24)$$

The reaction for  $\text{H}^+$  in biofilm segment  $[w, n]$  is:

$$\text{Reaction}_{\text{H}^+} = +K_1 \times C_{\text{NH}_4} b[w, n] - K_{-1} \times C_{\text{NH}_3} b[w, n] \times C_{\text{HH}} b[w, n]$$

$$\begin{aligned}
&+K_2 \times C_{HNO_2} b[w, n] - K_{-2} \times C_{NO_2} b[w, n] \times C_{HH} b[w, n] \\
&+K_3 \times C_{HNO_3} b[w, n] - K_{-3} \times C_{NO_3} b[w, n] \times C_{HH} b[w, n] + R_1 \quad (25)
\end{aligned}$$

### ***Reactions in the Pore Water Phase***

In the pore water, only acid-base equilibrium occurs. The formulation of these reactions are the same as for Equations 19-25, (except that they refer to the pore water instead of the biofilm, and therefore are not shown here). There is no biological reaction in the pore water ( $R_1$  or  $R_2$ ).

### **Model for the Denitrification Vessel**

The dynamic mass balance for  $NO_3$  in the denitrification tank is much simpler as it is assumed that it behaves as a continuously stirred tank reactor:

$$(VDN + VDNR) \frac{dC_{NO_3} DN}{dt} = L_R(C_{NO_3} I[w]) - C_{NO_3} DN \times (L_R + F) - R_1 DN \times VDNR \quad (26)$$

where  $L_R$  is the trickling rate and  $F$  is the rate of glucose solution fed to the denitrification tank.

Similarly, the dynamic mass balance for  $NO_2$  in the denitrification tank is:

$$(VDN + VDNR) \frac{dC_{NO_2} DN}{dt} = L(C_{NO_2} I[w]) - C_{NO_2} DN \times (L + F) + (R_1 DN - R_2 DN) \times VDNR \quad (27)$$

The dynamic mass balance for the  $C_6H_{12}O_6$  in the denitrification tank is:

$$VDNR \frac{dC_{COD} DN}{dt} = F(C_{COD}^{inlet}) - C_{COD} DN \times (L + F) - R_1 DN \times VDNR \times Stoich1 - R_2 DN \times VDNR \times Stoich2 \quad (28)$$

### ***Biodegradation kinetics in the denitrification tank***

A modified Michaelis-Menten kinetic is used to describe the biodegradation of nitrate and nitrite, as the kinetics are expected to be affected by the substrate concentrations.

$$R_1 DN = \frac{R_1 DN \max \times C_{NO_3} DN}{C_{NO_3} DN + K_{SNO_3}} \times \frac{C_{COD} DN}{C_{COD} DN + K_{SCOD}} \quad (29)$$

$$R_2 DN = \frac{R_2 DN \max \times C_{NO_2} DN}{C_{NO_2} DN + K_{SNO_2}} \times \frac{C_{COD} DN}{C_{COD} DN + K_{SCOD}} \quad (30)$$

in which  $R_1 DN \max$  is the maximum degradation rate expressed per unit of biofilm volume ( $\text{mol}_i \text{m}^{-3} \text{biofilm h}^{-1}$ ) and  $K_S$  is the half-saturation rate constant ( $\text{mol substrate m}^{-3} \text{biomass h}^{-1}$ ).





### **Denitrification filter setup and operating conditions**

Denitrification was carried out in a separate different reactor. The size of denitrification reactor was  $0.4\text{m} \times 0.4\text{m} \times 0.7\text{m}$  (height) and it was filled with  $0.03\text{ m}^3$  of the similar spherical porous ceramics as in the biotrickling filter, except that this kind was amended with cow bone (CB Porcelite®, AISIN TAKAOKA CO, LTD., Toyota, Aichi, Japan.). The packed bed was kept submerged and the circulation flow rate to and from the biotrickling filter sump was maintained at  $0.0075\text{m}^3\text{ h}^{-1}$ .

### **Analysis**

Ammonia gas was analyzed by detector tube. Liquid samples were analyzed for  $\text{NH}_3$ ,  $\text{NO}_2$ ,  $\text{NO}_3$  by Shimadzu ion chromatograph LC-VP and COD was checked by simple packet kit.

## **RESULTS AND DISCUSSION**

### **Determination of Model Parameters**

A number of model parameters, such as physicochemical constants were readily available from the literature, others have been roughly estimated and their values are in the process of being refined.

### Ammonia Treatment Performance (Pilot Biotrickling Filter)

The performance of the biotrickling filter removing ammonia was investigated by keeping the inlet concentration of ammonia at an average value of 26 ppm. The air flow was kept at a constant value of  $150 \text{ m}^3 \text{ h}^{-1}$ . The trickling rate (in a recycle mode) was kept  $0.015 \text{ m}^3 \text{ h}^{-1}$ . The results, shown in Figure 3. The removal of ammonia was essentially constant at 98%, except for selected values. At the same time, nitrate accumulation can be seen (Figure 4), though to a lesser extent than calculated from the ammonia supply indicating that some denitrification was occurring. Tuning of the denitrification tank volume and feed rate of COD is being undertaken.

**Figure 3.** Removal efficiency at average inlet ammonia concentration was 26 ppm and air flow was  $150 \text{ m}^3 \text{ h}^{-1}$ . Experimental data. Conditions were as described in the methods Section. (note that the reactor had been operated for several months without ammonia monitoring equipment, hence no data are shown prior to Aug. 1).

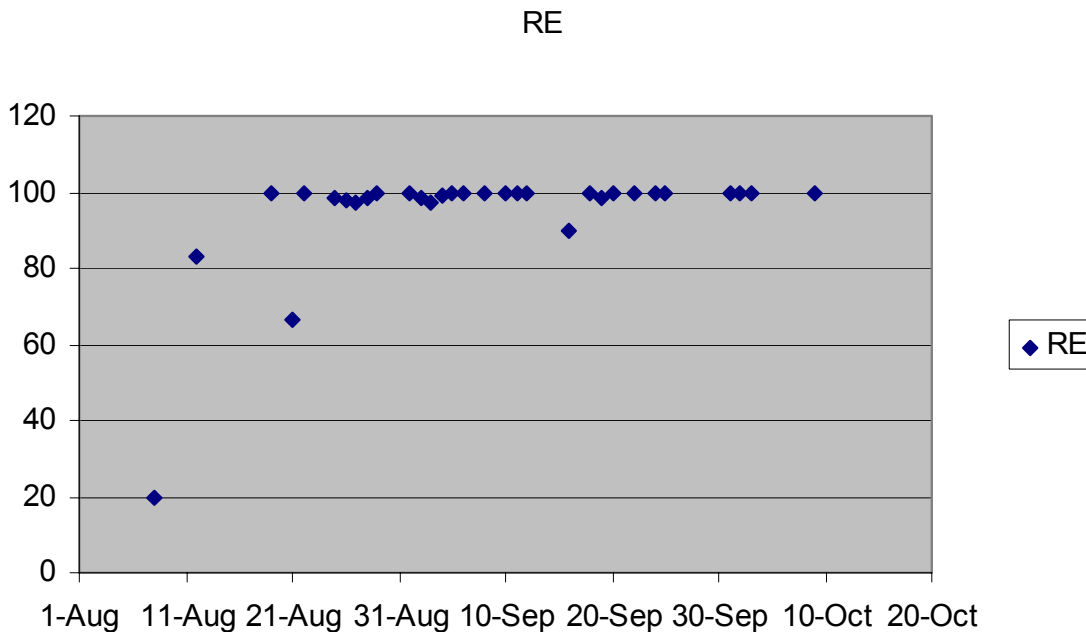
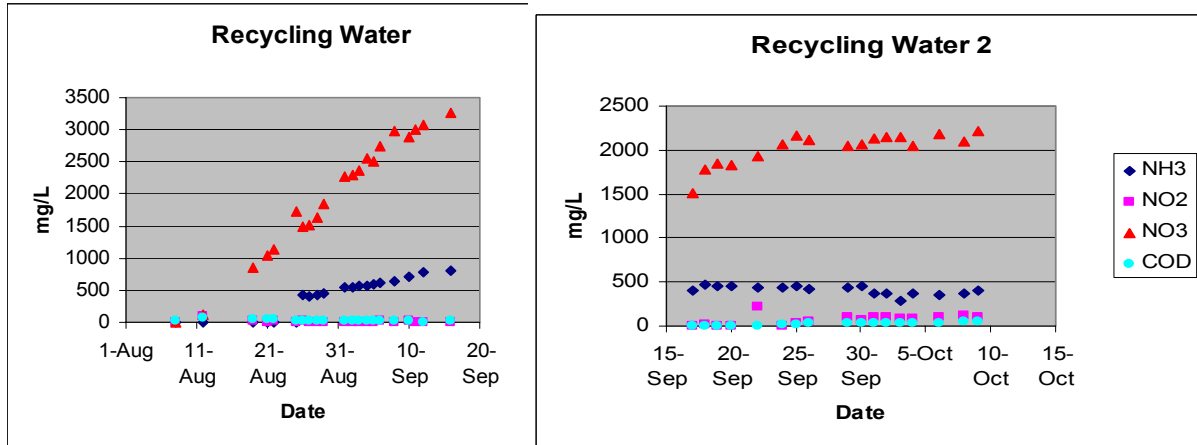


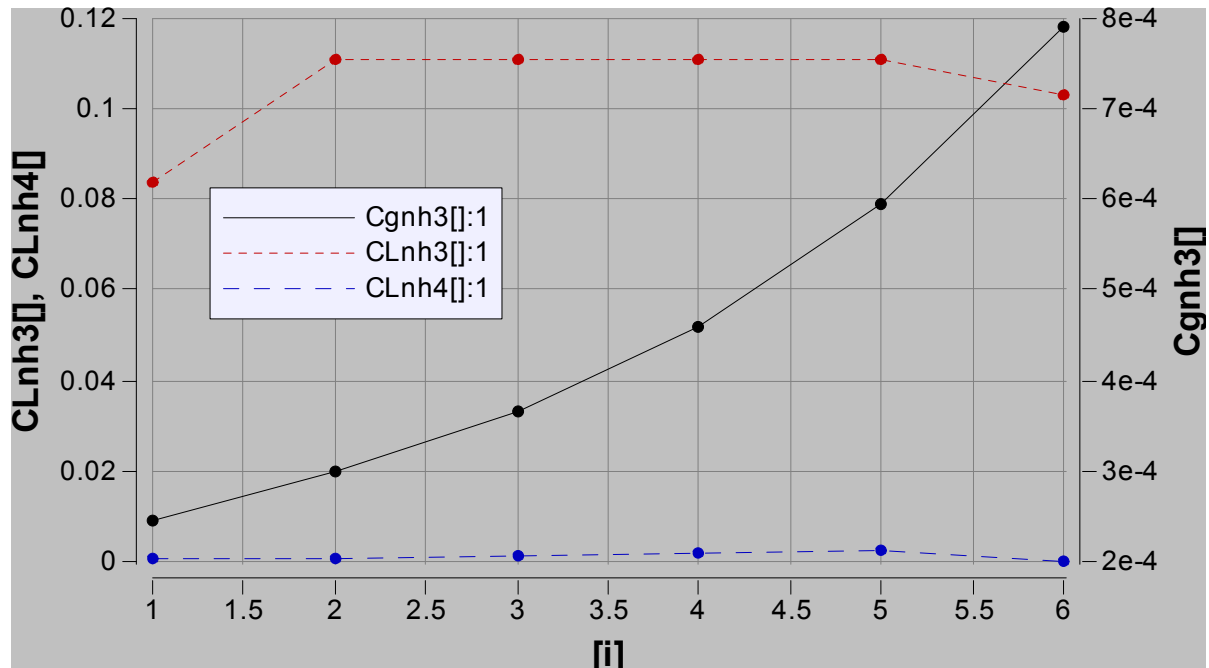
**Figure 4.** Liquid parameters for the pilot biotrickling filter. Conditions were as described in the methods Section and Figure 3.



### Model Simulations and Comparison with Field Performance

Model simulations are still ongoing. The model presented in this paper requires relatively large CPU time, and system of equations is relatively stiff. An example of simulation is shown in Figure 5, where the gaseous and liquid concentrations of ammonia and shown along the height of the reactor.

**Figure 5.** Axial profile of gaseous ammonia, liquid ammonia and ammonium. All concentrations are in moles  $m^{-3}$ , the x axis represents the finite elements for the numerical solution (left = top of reactor, right = bottom of reactor). Conditions and dimensions as in Methods Section.



Some difficulties were experienced with the model, and the code is being revised to ensure that there are no mistakes, and to possibly improve its user friendliness. As more simulations and updates become available, they will be posted at [http://www.engr.ucr.edu/~mdeshuss/awma\\_nh3.htm](http://www.engr.ucr.edu/~mdeshuss/awma_nh3.htm)

## CONCLUDING REMARKS

In the present paper, a conceptual model of a biotrickling filter was developed. The model attempted to include all relevant processes that occur during treatment. At this time, the model is still being refined and validation is pending. When fully developed, the model is expected to be a significant support for the design and operation of biotrickling filter for ammonia control.

## ACKNOWLEDGEMENTS

The support by Aisin Takaoka Co., Ltd, Japan is greatly acknowledged.

## NOMENCLATURE

- A (m<sup>2</sup> m<sup>-3</sup>) interfacial area
- C<sub>ib</sub> (mol m<sup>-3</sup>) concentration of substance i in the biofilm
- C<sub>iDN</sub> (mol m<sup>-3</sup>) concentration of substance i in the Denitrification tank.
- C<sub>ig</sub> (mol m<sup>-3</sup>) concentration of substance i in the gas
- C<sub>il</sub> (mol m<sup>-3</sup>) concentration of substance i in the liquid
- C<sub>ip</sub> (mol m<sup>-3</sup>) concentration of substance i in the pore
- D<sub>i</sub> (m<sup>2</sup> h<sup>-1</sup>) effective diffusion coefficient of substance (D<sub>c</sub>) or oxygen (D<sub>o</sub>)
- F (m<sup>3</sup> h<sup>-1</sup>) feed flow rate
- G (m<sup>3</sup> h<sup>-1</sup>) airflow rate
- H<sub>d</sub> dynamic liquid holdup
- H<sub>i</sub> Henry coefficient of substance i
- H<sub>s</sub> static liquid holdup
- J<sub>bi</sub> (mol m<sup>-2</sup> h<sup>-1</sup>) the flux of the substance i into the biofilm
- J<sub>gi</sub> (mol m<sup>-2</sup> h<sup>-1</sup>) the flux of the substance i from the liquid into the gas phase
- K<sub>j</sub> (mol m<sup>-3</sup> h<sup>-1</sup>) maximum biodegradation rate for process j

- $K_{Iji}$  (mol m<sup>-3</sup>) inhibition constant of substance i in process j  
 $K_m$  (mol m<sup>-3</sup>) Michaelis-Menten constant of substance  
 $K_o$  (mol m<sup>-3</sup>) oxygen half-saturation constant  
 $K_{ga}$  gas-liquid mass transfer coefficient multiplied by specific interfacial area  
 $K_{Sji}$  (mol m<sup>-3</sup>) half-saturation constant of substance i in process j  
 $L_R$  (m<sup>3</sup> h<sup>-1</sup>) trickling rate for denitrification  
 $N$  (-) number of biofilm subdivisions in each layer (here  $N = 10$ )  
 $n$  biofilm subdivisions ( $1 \leq n \leq N$ )  
 $R_j$  (mol m<sup>-3</sup> h<sup>-1</sup>) degradation rate of process j  
 $R_{jDN}$  (mol m<sup>-3</sup> h<sup>-1</sup>) degradation rate of denitrification process j  
 $t$  (min) time  
 $T$  (m) biofilm thickness  
 $V$  (m<sup>3</sup>) total reactor volume  
 $VDN$  (m<sup>3</sup>) volume of liquid for denitrification  
 $VDNR$  (m<sup>3</sup>) volume of packing for denitrification  
 $V_{gw}$  (m<sup>3</sup>) volume of the gas subdivision  
 $V_{lw}$  (m<sup>3</sup>) volume of the liquid subdivision  
 $V_{jm}$  (mol m<sup>-3</sup> h<sup>-1</sup>) maximum degradation rate for process j  
 $V_{pw}$  (m<sup>3</sup>) volume of the pore subdivision  
 $W$  number of layer subdivisions (here  $W = 10$ )  
 $w$  biofilter layer subdivisions: ( $1 \leq w \leq W$ )

### ***Greek Symbols***

(m) thickness of one biofilm subdivision ( $\delta = T/N$ )

### **Subscripts**

i substance

j process

## REFERENCES

- (1) Zhu, S.; Chen, S. Impacts of Reynolds Number on Nitrification Biofilm Kinetics; *Aquacultural Engineering* **2001**, *24*, 213-229
- (2) Schulthess, R.v.; Gujer, W. Release of Nitrous Oxide (N<sub>2</sub>O) from Denitrifying Activated Sludge: Verification and Application of a Mathematical Model; *Wat Res.* **1996**, *30*, 521-530
- (3) Carrera, J.; Gabriel, D.; Vicent, T.; Lafuente, J. Modeling the Nitrification Process Considering the Inhibition by Free Ammonia and Free Nitrous Acid; **2003** (draft manuscript, personal communication)
- (4) Dunn, I. J.; Heinzle, E.; Ingham, J.; Prenosil, J. E. Biological Reaction Engineering; VCH: Weinheim, Germany, **1992**; p 438.
- (5) Ingham, J.; Dunn, I. J.; Heinzle, E.; Prenosil, J. E. Chemical Engineering Dynamics; 2nd edition VCH : Weinheim, Germany, **1994**; p 701.
- (6) Siegrist, H.; Gujer, W. Demonstration of Mass Transfer and pH Effects in a Nitrifying Biofilm; *Wat Res.* **1987**, *21*, 1481-1487
- (7) Hagopian, D.S; Riley, J.G. A Closer Look at the Bacteriology of Nitrification; *Aquacultural Engineering* **1998**, *18*, 223-244
- (8) Xie, Y; Biswas, N; Bewtra, J.K. Nitrification and Denitrification in Water and Soil Environments; *Intern. J. Environ. Studies.* **1999**, *56*, 451-474
- (9) Dalsgaard, T; Revsbech, N.P. Regulating Factors of Denitrification in Trickling Filter Biofilms as Measured with the Oxygen / Nitrous Oxide Microsensor; *Microbiology Ecology.* **1992**, *101*, 151-164
- (10) Zhu, S.; Chen, S. Impacts of Temperature on Nitrification Rate in Fixed Film Biofilters; *Aquacultural Engineering* **2002**, *26*, 221-237
- (11) *Handbook of Chemistry and Physics*, 84<sup>th</sup> Edition; CRC Press: Boca Raton, Florida, **2003**
- (12) Montgomery, J.H. *Groundwater Chemicals Desk Reference*, 3<sup>rd</sup> Edition; CRC Lewis Publisher: Boca Raton, Florida, **2000**